AGU ADVANCING EARTH AND SPACE SCIENCES

Water Resources Research

RESEARCH ARTICLE
10.1029/2023WR035840

Beyond the Wedge: Impact of Tidal Streams on Salinization of Groundwater in a Coastal Aquifer Stressed by Pumping and Sea-Level Rise

M. C. Hingst[1], R. M. Housego[1,2], C. He[3], B. J. Minsley[4], L. B. Ball[4], and H. A. Michael[1,5]

[1]University of Delaware Department of Earth Sciences, Newark, DE, USA, [2]Pennsylvania State University Department of Geosciences, State College, PA, USA, [3]Delaware Geological Survey, Newark, DE, USA, [4]U.S. Geological Survey, Geology, Geophysics, and Geochemistry Science Center, Denver, CO, USA, [5]University of Delaware Department of Civil and Environmental Engineering, Newark, DE, USA

Key Points:

- Presence of a saltmarsh inverts the freshwater-saltwater interface in our study location
- Tidal streams contribute substantially to salinization of inland groundwater
- Concentrated pumping led to more intensive salinization than widespread pumping

Supporting Information:

Supporting Information may be found in the online version of this article.

Correspondence to:

H. A. Michael,
hmichael@udel.edu

Citation:

Hingst, M. C., Housego, R. M., He, C., Minsley, B. J., Ball, L. B., & Michael, H. A. (2024). Beyond the wedge: Impact of tidal streams on salinization of groundwater in a coastal aquifer stressed by pumping and sea-level rise. *Water Resources Research*, *60*, e2023WR035840. https://doi.org/10.1029/2023WR035840

Received 12 JUL 2023
Accepted 3 JUL 2024

Abstract Saltwater intrusion (SWI) is a well-studied phenomenon that threatens the freshwater supplies of coastal communities around the world. The development and advancement of numerical models has led to improved assessment of the risk of salinization. However, these studies often fail to include the impact of surface waters as potential sources of aquifer salinity and how they may impact SWI. Based on field-collected data, we developed a regional, variable-density groundwater model using SEAWAT for east Dover, Delaware. In this location, major users of groundwater from the surficial aquifer are the City of Dover and irrigation for agriculture. Our model includes salinized marshland and tidal streams, along with irrigation and municipal pumping wells. Model scenarios were run for 100 years and included changes in pumping rates and sea-level rise (SLR). We examined how these drivers of SWI affect the extent and location of salinization in the surficial aquifer by evaluating differences in chloride concentration near surface waters and the subsurface freshwater-saltwater interface. We found the presence of the marsh inverts the typical freshwater-saltwater wedge interface and that the edge of the interface did not migrate farther inland. Additionally, we found that tidal streams are the dominant pathways of SWI at our site with salinization from streams being exacerbated by SLR. Our results also show that spatial distribution of pumping affects both the magnitude and extent of salinization, with an increase in concentrated pumping leading to more intensive salinization than a more widely distributed increase of the same total pumping volume.

1. Introduction

As sea level continues to rise and demand for freshwater increases, coastal groundwater resources face increasing risk of contamination from saltwater intrusion (SWI). Although it may seem that SWI is a relatively new problem brought on by anthropogenic climate change and increased groundwater withdrawals, many coastal areas have been dealing with SWI issues for over a hundred years (Back & Freeze, 1983; Barlow & Reichard, 2010; Carr, 1969). For as long as SWI has been an issue there have been extensive studies on the physics, extent, and future projections of SWI (e.g., Chang & Clement, 2012; Goswami & Clement, 2007; Kohout, 1960; Meyer et al., 2019; Todd, 1953). The accessibility of modern computing has increased the quantity and quality of numerical SWI models and studies that assess the impact of different aquifer hydraulic properties on SWI (e.g., Bakker, 2003; Bobba, 1993; Guo & Langevin, 2002; Langevin et al., 2008). However, many of these SWI studies, particularly of the regional scale, fail to capture the complete hydrologic system by disregarding surface water connections to groundwater.

Most previous modeling studies of SWI were constructed assuming a defined and abrupt boundary between the land (freshwater) and sea (saltwater), similar to that of the benchmark Henry Problem (Pinder & Cooper, 1970). This setup resembles sandy beaches and allows for the clear formation of a typical saltwater wedge beneath the surface along the coastline. However, a substantial portion of the global coastline is fringed by saltmarshes with estimates varying from 2.2 to 40 Mha (McOwen et al., 2017; Xin et al., 2022). Saltmarshes are characterized by layers of fine, low-permeability sediments and are regularly inundated by high tides, resulting in brackish to saline porewater (Guimond & Tamborski, 2021). In recent years there has been an increased interest in studying the hydrology of saltmarshes (Guimond et al., 2020; Xin et al., 2022). Because it is difficult to maintain field equipment or install wells in saltmarsh areas due to the saturated nature of the sediments and frequent inundation, few studies have examined saltmarsh impacts on deeper groundwater, especially as saltmarshes pertain to SWI in

the subsurface. The connectivity between rivers and streams to aquifers has been extensively studied (Brunner et al., 2010; Kalbus et al., 2006; Nield et al., 1994; Sophocleous, 2002), but the potential for surface waters to act as pathways for salinization has been largely overlooked.

Groundwater modeling studies that have incorporated tidal streams or marshes and salinity have primarily focused on understanding the flow dynamics, water balance and salinity distributions within the surface waters themselves or in the aquifer within the immediate vicinity. There is a need for studies which evaluate salinity and flow dynamics of aquifers in large-scale systems where groundwater and surface water are interconnected, and pumping is occurring. For example, Michot et al. (2011) used modeling to examine the water budget and water quality, including salinity, in the Taylor River in the Everglades wetlands in the United States. Their model focused on the contribution of flow and salinity from groundwater into the stream, and only assessed salinity changes within the stream itself, not within the aquifer. Werner and Lockington (2006) and Lenkopane et al. (2009) modeled the impact of tidal fluctuations on the salinity in the adjacent aquifer. Both studies found there was greater change in the salinity at the top of the aquifer compared to the base, shedding light on the importance of streams as sources of salinity in groundwater salinization. However, the employed models were small (<200 m in length), and did not include effects of pumping wells, limiting the understanding of flow and salinity dynamics of more complicated, real-world systems. A study by Xiao et al. (2019) modeled the flow dynamics in a coastal aquifer beneath a marsh creek, with results focusing on submarine groundwater discharge and flow dynamics of the intertidal zone. As the marsh was set to a no-flow boundary, it did not contribute water or salt to the model area which would be expected. All these studies ran models on short time scales, examining changes over seasonal or annual periods. The only study the authors could find that modeled the impact of a tidal stream on SWI over a longer period is Masterson and Garabedian (2007). This study used a simplified model to represent a tidal stream and aquifer on Cape Cod, Massachusetts, USA, and assess the impacts sea-level rise (SLR) within a tidal stream have on the subterranean freshwater lens. As pointed out by the authors of that study, the cape area is more hydrogeologically similar to an island than a continental coastal aquifer, with saltwater found beneath a lens of freshwater. Like the previously mentioned studies, Masterson and Garabedian did not incorporate pumping wells. These studies collectively underscore the complexities of groundwater-surface water interactions and highlight the need for more comprehensive models that consider longer timescales, broader spatial extents, and the influence of pumping wells to better understand salinity dynamics in coastal aquifers.

Researchers have shown that the salt front (usually defined as the 250-ppm chloride contour) in rivers and estuaries is expected to migrate inland with SLR in most coastal environments (Cook et al., 2023; Costa et al., 2023; Rice et al., 2012; Yuan et al., 2015). Separate studies have analytically assessed how increased pumping could draw water out of rivers, leading to landward movement of the surface salt front (Peters et al., 2022). A study by Kazakis et al. (2019) proposed a revised version of the often-used GALDIT assessment method which calculates risk of SWI based on geologic and hydrogeologic parameters. The hybrid GALDIT-SUSI incorporated risk of SWI from connected surface water bodies into the assessment criteria and found that doing so provided more accurate delineation of areas of high and low risk to SWI (Kazakis et al., 2019). Recently, there have been some field-based and analytical studies that have looked at increasing salinity of groundwater in connection with saline rivers and canals (Setiawan et al., 2023; Shalem et al., 2019), but there remains a lack of modeling studies, and corresponding field data to validate the models, that examine the connection between surface water, groundwater, and salinization.

The impacts of the spatial distribution of pumping on SWI have primarily been studied in the context of pumping optimization models which use algorithms to maximize groundwater extraction while limiting salinization (e.g., Cheng et al., 2000; Dhar & Datta, 2009; Mantoglou, 2003). However, the needs of individual users are often not considered in optimization studies. Whereas a municipality may be able to adjust its wells to optimal pumping rates to still meet demands, farmers typically only have a single well on their property with pumping controlled by the water demand of their crops. Thus, if water demand increases, all farmers in the area will need to pump water at the same time. In regions of established irrigated agriculture, implementing the findings of optimization studies that prescribe unevenly reduced pumping rates for select water users is difficult. Therefore, when evaluating SWI in regions with competing water users, it could be beneficial from a management standpoint to assess the overall risk of salinization across the system and its potential evolution in the future, rather than delving into intricacies of optimal pumping rates.

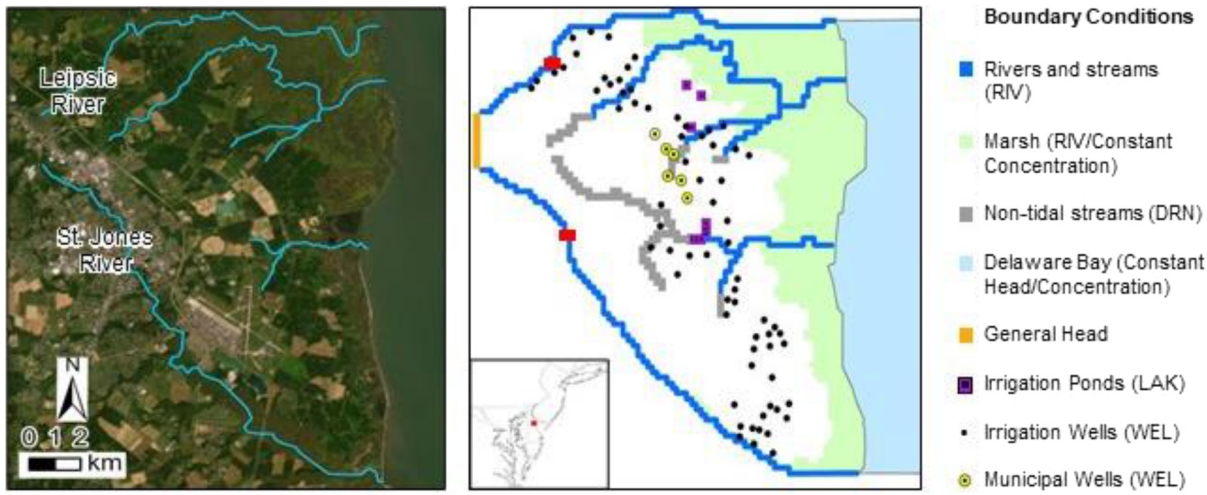

Figure 1. (left) Aerial map of study area with tidal streams and rivers incorporated into the model highlighted in blue (ESRI Basemap, 2009). (right) Overview of the layout of boundary conditions used in the model. Red rectangles mark the inland extent of the reach of the tide based on the location of a dam on the Saint Jones River and inundation mapping for the Leipsic River (Delaware Coastal Inundation Map, 2017); sea-level rise was not applied further upstream of these marks in the model.

In this study, we use Dover, Delaware, as an example of a hydrologic setting in which irrigated agricultural operations are transversed by tidal streams and fringed by coastal marshes. We apply a numerical model to assess the impact of surface water bodies, including tidal streams and a saltmarsh, on the extent of salinization of groundwater and how the spatial distribution of pumping can affect the pathways of SWI. Irrigated agricultural operations transversed by tidal streams or fringed by coastal marshes can be found in coastal areas around the world, such as along the East and Gulf Coasts of the United States (Fenstermacher et al., 2014; Sadeghi et al., 2019), the Fens region in the UK (Moulds et al., 2023), around Europe (Raats, 2015), and China (Han & Currell, 2022). This is especially true for the Delmarva Peninsula on the east coast of the United States, where which most of the land is cropland (Fenstermacher et al., 2014). On the west side of the peninsula in Maryland, farmland has already been abandoned due to flooding and salinization from SLR (Tully et al., 2019). The eastern side of the peninsula in Delaware has yet to face such a dire situation; however, given its low-lying elevation, the rate of SLR, and sole reliance on groundwater, Delaware is vulnerable to SWI in the near future. The results from this study shed light on the impact surface waters can have on SWI and the considerations for managing SWI in coastal environments where competing groundwater withdrawals are in proximity to tidal channels and marshes.

2. Materials and Methods

2.1. Study Area

The area of east Dover, Delaware, USA, serves as the basis for this study because it is fringed by marshland and transected by tidal streams (Figure 1). Dover is located on the Delmarva Peninsula in the Mid-Atlantic region of the United States, which is experiencing some of the fastest rates of relative SLR, about twice the global average, due to glacio-isostatic adjustment (Miller et al., 2013). Projections range between 0.5 and 1.8 m of SLR by 2100 in this region, with an average estimate of 1 m (DNREC, 2012; Miller et al., 2013). The maximum elevation in the study area is about 21 m above mean sea-level, and the average elevation is approximately 9.8 m. This low elevation and high rate of SLR increases the vulnerability of the area to SWI.

The study area is underlain by the North Atlantic Coastal Plain which is composed of unconsolidated sediments that were deposited between the Late Cretaceous and Pleistocene (Olsson et al., 1988). These sediments form multiple, layered aquifers and confining units. Within the study area, the main aquifers are part of the Calvert Formation of the Chesapeake Group which has been reported on extensively by Richards (1967), Kidwell (1984), and Ator et al. (2005). In general, the units of the Calvert Formation dip and thicken to the southeast, off the coastline, with some sub-cropping out around the northwest corner of the study area (Mclaughlin & Velez, 2006). The present study focuses on the surficial Columbia aquifer composed of fine to coarse sand with discontinuous lenses of gravel and mud beds (Andres, 2004; Mclaughlin & Velez, 2006). Some of the mud beds create localized

confining conditions, but in general, the aquifer is described as unconfined (Andres & Klingbeil, 2006). Where present, the thickness of the surficial aquifer varies from 2 to 35 m (Andres et al., 2023; McLaughlin et al., 2009). The water table generally follows land surface elevation and is within a few meters of the surface (Andres et al., 2023; Martin & Andres, 2008). The hydraulic conductivity of the aquifer ranges from 0.25 to 100 m/d with an average of 12.8 m/d, based on 47 measurements from around Kent County (location of the study area; Andres et al., 2019).

Groundwater is the primary source of freshwater for municipal, domestic, industrial, and irrigation uses. While the city of Dover pumps the majority of its municipal water supply from the deeper parts of the Calvert Formation, the Cheswold (30%) and Piney Point (60%) aquifers, it obtains approximately 10% of its supply from the Columbia aquifer (Hingst et al., 2022). Based on data from 2011 to 2020, supplied by the Delaware Department of Natural Resources and Environmental Control (DNREC), daily pumping from the Columbia averaged 1,232 cubic meters. The Columbia supplies approximately 90% of all irrigation water in the area which equates to approximately 9,308 cubic meters per day. Most farmers use wells to obtain their irrigation water, and a few withdraw water from irrigation ponds. These ponds are located adjacent to marshes or streams and were created by excavating down into the top of the Columbia, making them groundwater-fed (Hingst et al., 2022). Dover's municipal wells completed in the Columbia aquifer wells in Dover are located in the center of the study area, near the irrigated cropland, which concentrates a large volume of pumping around two of the tidal streams. There are DNREC records for 427 domestic wells within the study area; however, these wells were excluded from the model due to their low pumping rates (i.e., approximately 1 m^3/d).

2.2. Model Set-Up

2.2.1. Model Structure, Properties and Boundary Conditions

Waterlook Hydrogeologic (2023) The model was developed using Waterloo Hydrogeologic Visual MODFLOW Flex© Version 8.0, and run using SEAWAT V4 (Langevin et al., 2008), and is an idealized representation of the Columbia aquifer underlying the area east of the Dover urban area. It was constructed with a finite difference grid consisting of 100 rows and 91 columns, with each cell being 200 × 200 m. A Digital Elevation Model of the surface, collected via lidar was used as the model surface (Airborne Topographic LiDAR Report, 2015). To avoid cell connectivity issues due to differences in elevation, a uniform thickness of 16 m, the average thickness of the aquifer in the area of interest along the coast, was applied by subtracting 16 m from the surface to create the bottom elevation profile. The model was divided into four layers of equal thickness (4 m). The thickness and slope of an aquifer have been previously shown to impact the extent of SWI (e.g., Abd-Elhamid et al., 2019; Walther et al., 2017), but as the main purpose of this paper is to understand salinization processes generally, with a focus on the impacts of surface water bodies on SWI into groundwater, these impacts were not assessed in the current paper. To test sensitivity to discretization, the model was also divided into 8 layers of 2-m thickness. There was only a 1.92% difference in total mass flux of salt between the 4-layer and 8-layer setup after calibration was complete, and so the 4-layer structure was used to reduce computational time. The Leipsic and Saint Jones Rivers serve as the inland boundaries along the north and southwest sides. The head for the inland general head boundary was selected based on the maximum water level elevation west of the model, across the Delmarva Peninsula. At its widest points, the model spans 19.5 km north–south and 18 km east–west. The offshore boundary extends approximately 4.4 km offshore into the Delaware Bay.

Initial hydraulic properties and boundary condition values were based on collected field data and values used in the east Dover groundwater model by He and Andres (2018), then adjusted manually during calibration (Table 1). A final horizontal hydraulic conductivity value of 20 m/d was used for the inland area in layer 1 and in all of layers 2, 3, and 4, which is within the range of measured values for the Columbia aquifer (Andres et al., 2019). A value of 1 m/d was used in layer 1 for the marsh and Delaware Bay area to represent higher levels of silt and clay found in wetland sediments. A 10:1 ratio for horizontal to vertical hydraulic conductivity was used for the entire model. All layers were assigned to behave as confined with constant transmissivity and storage coefficient to mitigate issues with drying and rewetting of cells, but a specific storage of 0.05 was applied to the top layer to mimic the specific yield of an unconfined aquifer. Visual MODFLOW Flex© multiplies the specific storage by the layer thickness (4 m) which yielded a primary storage coefficient value of 0.2 for the top layer.

An annual average net recharge rate of 150 mm/yr, approximately 13% of annual precipitation (Delaware Climate Office), was applied over the entirety of the land cells in the model. This is 4 mm less than the average net

Table 1
Values of Model Hydraulic Properties

Property	Aerial extent	Layers	Value
Hydraulic conductivity	Inland	All layers	20 m/d (K_x, K_y); 2 m/d (K_z)
Hydraulic conductivity	Marsh/Delaware Bay	1	1 m/d (K_x, K_y); 0.1 m/d (K_z)
Storage coefficient	Entire model	1	0.05
Storage coefficient	Entire model	Layers 2–4	0.0002
Total porosity	Entire model	All layers	0.3
Effective porosity	Entire model	All layers	0.15
Dispersivity	Entire model	All layers	Horizontal 25 m, Longitudinal 2.5 m
Diffusion coefficient	Entire model	All layers	1.48 E−4 m^2/d

recharge (154 mm/yr) that was calibrated in the east Dover groundwater flow model by He and Andres (2018). Because this is a net recharge, it is assumed that it accounts for any return flow from irrigation back into the aquifer. The recharge boundary was assigned a chloride concentration of 15 mg/L based on average groundwater chloride concentrations in the Columbia aquifer as measured by Andres et al. (2023).

Constant head and constant concentration boundary conditions were assigned to cells within the Delaware Bay. To assess the impact of relative SLR on SWI, an initial head of 0 m was applied. The Delaware Bay is a mix of freshwater from the Delaware River and saltwater from the Atlantic Ocean and reported salinity values near the study area average approximately 17.5 practical salinity units (PSU) (Galperin & Mellor, 1990; NOAA). A chloride concentration of 9,700 mg/L, half that of seawater, and corresponding density of 1,012.5 kg/m^3, was used in the model. Chloride concentration was not increased with increasing sea level of the boundary conditions representing the Delaware Bay, tidal streams, or marshes, though that would be expected to occur as the salt front migrates inland. Our approach is conservative and focuses on the pathways of salinization rather than precision of future salinity levels.

In order for the marsh area to represent a source of salt in the model, river boundary conditions were applied allowing for the inflow and outflow of water. The surface elevation of the marsh is relatively low (<2 m) and is frequently inundated during high tide, thus heads for all marsh cells were set to 0 m, the same head as the Delaware Bay cells. The average tidal range varies between approximately −0.6 and 1.1 m msl (Hingst et al., 2022). An initial conductance value of 130 m^2/d was calculated for the marsh area using a bed thickness of 3.1 m and conductivity of 0.01 m/d. The bed thickness was based on a monitoring well installed by Hingst et al. (2022) at the edge of the marsh, and the conductivity was taken from Guimond and Michael (2021). A final conductance value of 35 m^2/d was assigned following calibration. Additionally, because of the fine-grained nature of marsh sediments and frequent inundation with seawater, a constant chloride concentration of 9,000 mg/L was also applied to the marsh area.

River boundary conditions were applied to perennial streams and rivers within the model. Portions of the streams within the marsh area were assigned heads of 0 m and concentrations of 9,000 mg/L to match that of surrounding cells and limit numerical instabilities. Heads and concentrations were then graded (i.e., increasing head, and decreasing concentrations moving inland) based on field measurements reported by Hingst et al. (2022) and data from the National Estuarine Research Reserve Systems (NERRS) (2003). If no field measurements were available for streams, heads were estimated to be between 1.15 and 1.5 m below the top of cell and adjusted accordingly during calibration. Conductance values were initially calculated assuming a hydraulic conductivity of 0.0864 m/day (Calver, 2001), a riverbed thickness of 1 m and polyline length in the cell. Conductance values were then adjusted manually while preserving the polyline length differences (i.e., all increased or decreased by the same factor) during calibration, resulting in varied conductances for each cell. Ephemeral streams which were determined based on inundation maps were modeled as drain boundaries with heads set to 1.25 m below the top of the cell (Delaware Coastal Inundation Map, 2017).

DNREC provided information on the location, construction, and pumping rates for the six city of Dover wells completed in the Columbia aquifer. A 10-year (2011–2020) average of total annual pumped volumes from these six wells was used to calculate the daily pumping rates for these six well boundary conditions in the model.

Because DNREC records for irrigation wells are limited compared to records for the municipal wells, modeled irrigation wells and pumping rates were based on values in a groundwater use study by Brinson (2023) which assumed one well per center-pivot sprinkler as identified through aerial imagery, and an average annual water usage of 652 m^3/acre. Sixty-nine irrigation wells were included in the model, with screens extending from 6 m below the surface to 0.5 m above the bottom of the model base. An average pumping rate of 1.79 m^3/day/acre irrigated land was applied. Total daily pumping rates for wells ranged from 17.8 to 527 m^3/d based on the crop area associated with each well as determined by Brinson (2023). In addition to the irrigation wells, five known irrigation ponds were included in the model. The ponds were simulated using lake boundary conditions. DNREC did have sufficient pumping records for the ponds and so the averaged heads and leakance values of the ponds were adjusted during calibration. Pumping from domestic wells was deemed to be insignificant based on the low pumping rates (generally <0.05 m^3/day) of such wells.

2.2.2. Calibration

Heads were calibrated to fit the current water table elevation map published by the Delaware Geological Survey in 2005 and averaged water levels from observation wells within the area (Figure S1 in Supporting Information S1). The observations wells used for calibration represent most monitoring wells completed in the Columbia aquifer and monitored by the Delaware Geological Survey. Observation wells that were not included were either those located adjacent to the municipal pumping wells and had skewed average heads from strong pumping signals or were located within the same grid cell as another well that was used. In the case of the latter, the well with a more complete record was chosen for calibration. The heads from the observation wells used during calibration were based on averages from up to 20 years of measurements. A review of historic water levels beginning with records from the 1970s did not indicate any discernible regional change in water levels in the Columbia aquifer which agrees with Andres et al. (2023). Monitoring wells are located primarily in the center of the model area, among the irrigated agricultural land and near the municipal pumping wells. The clustered location of the observation wells around the center of the model not only limited the accuracy to which heads could be calibrated in the northern and southern portions of the model but also limits the accuracy of water levels in the map that were used as comparison. Additionally, as most of the pumping and tidal streams are also located in the center of the model, deviation of the modeled head contours and mapped contours in the southern portion of the model was not considered to be of high importance. After steady-state conditions were achieved in the model, irrigation wells were pumped for 50 years and municipal wells for 25 years, the average length of time each respective type of well has been in operation. Measured heads were compared to model-calculated heads and had a R^2 value of 0.94 with a Root Mean Square Error (RMSE) of 0.28 and normalized RMSE of 8.18% (Figure S1 in Supporting Information S1).

Due to insufficient field salinity data available in the model area, specifically in the marsh area, chloride concentrations in the model could not be calibrated. Instead of point calibration, the resulting chloride distribution from the head calibration was qualitatively compared to cross-sectional resistivity models derived from an airborne electromagnetic (AEM) survey over the study area conducted by the U.S. Geological Survey (USGS) during the summer of 2022 (Figure 2) (U.S. Geological Survey, 2024). Bulk resistivity is strongly dependent on the pore water resistivity (or its inverse, fluid conductivity) (e.g., Archie, 1947) as well as lithology. In this relatively homogeneous aquifer with large contrasts in porewater salinity, the resistivity structure is expected to primarily reflect contrasts in salinity (Fitterman & Deszcz-Pan, 1998). While bulk resistivity is indirectly related to pore water salinity, AEM surveys have the advantage of providing spatially extensive and high-resolution information at depth along flight profiles to support model calibration.

2.2.3. Model Scenarios

Eight scenarios of varied pumping and sea level were run, each for 100 model years (Table 2). Scenario *A* was run using current pumping rates and no SLR to establish a baseline. Climate models predict that while total annual precipitation in the study area is likely to increase due to climate change, precipitation during summer months—when irrigation occurs—is likely to decrease and when combined with higher predicted temperatures that would likely lead to increased evapotranspiration (USGCRP, 2017). Scenario *B* addressed this situation by increasing irrigation pumping by 25%. To assess the impact that distribution of pumping has on SWI, scenario *C* incorporated an increase in municipal pumping by the same total volume as in scenario *B*, while keeping irrigation pumping at baseline values; this meant municipal well pumping rates were increased by 289%. Currently,

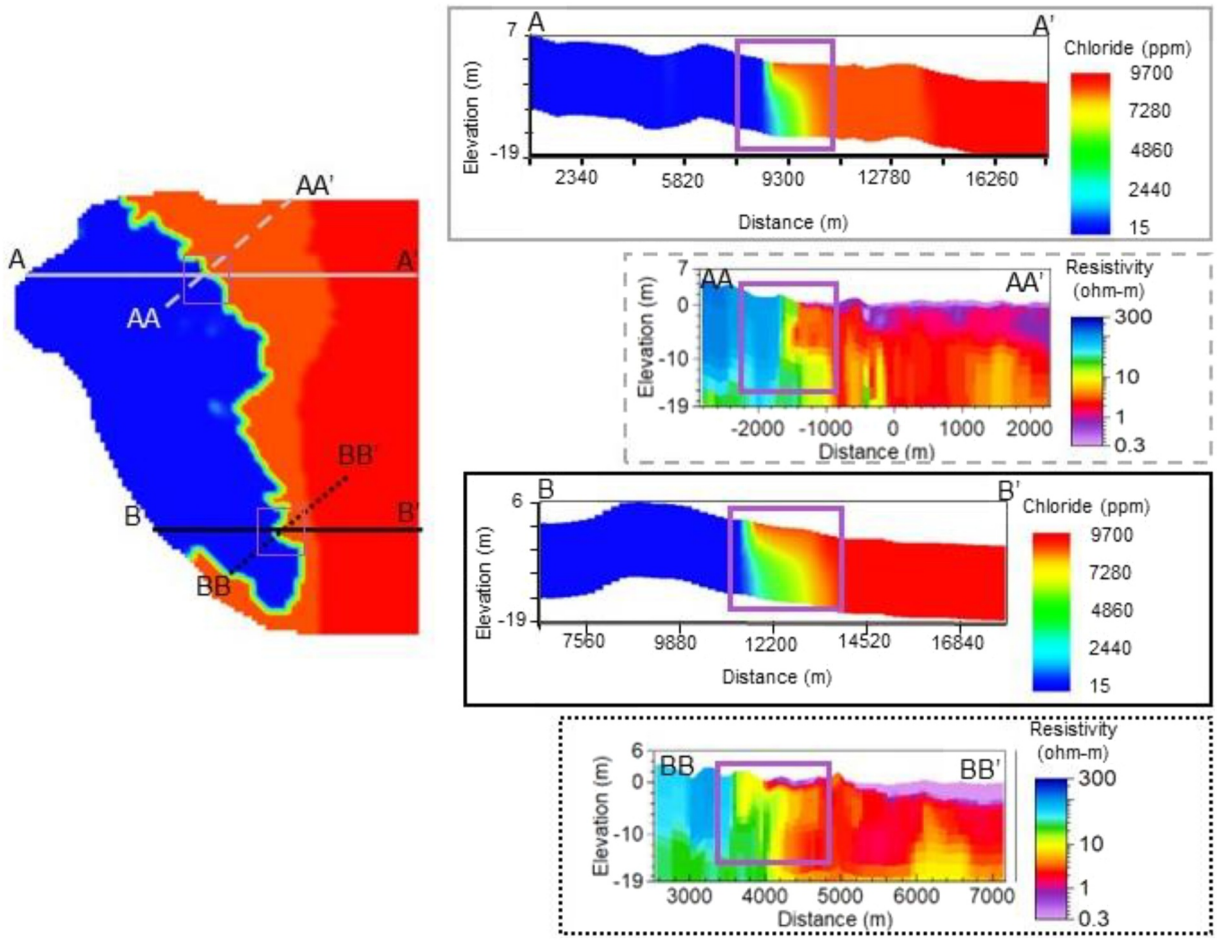

Figure 2. Comparison between chloride distribution in model at present day conditions compared to the airborne electromagnetic (AEM) survey. Cross-sections from the model (A–A' and B–B') intersect the AEM cross-sections (AA–AA' and BB–BB') at the edge of the marsh. This intersection is highlighted by the purple squares on the cross-sections.

municipal wells utilize approximately 10% of their total cumulative permitted maximum withdrawal limit of 3 million gallons per day (11,356 m^3). In the last pumping scenario (*D*), municipal wells were increased proportionally (i.e., by the same percentage), based on current average pumping rates to the permitted daily maximum limit. All these scenarios were then run again with the addition of SLR applied (Scenarios A-SLR, B-SLR, C-SLR, D-SLR). To balance the gradual increase in sea-level and acceptable run times, SLR was simulated by

Table 2
Pumping Amounts and Sea Level for Model Scenarios

Scenario	Scenario description	Total irrigation pumping (wells and ponds) [m^3/d]	Total municipal pumping [m^3/d]	Starting sea level [m]	Ending sea level [m]
A	Current pumping rates	9,308	1,232	0	0
B	Increased irrigation	11,635	1,232	0	0
C	Increased municipal pumping by 289%	9,308	3,559	0	0
D	Maximum municipal pumping	9,308	11,356	0	0
A + SLR	SLR + current pumping rates	9,308	1,232	0	1
B + SLR	SLR + increased irrigation by 25%	11,635	1,232	0	1
C + SLR	SLR + increased municipal pumping by 289%	9,308	3,559	0	1
D + SLR	SLR + maximum municipal pumping	9,308	11,356	0	1

increasing the heads in the Delaware Bay, rivers, and marsh by 1 m over 20 stress periods, which equated to 0.05 m per 5 model years. Chloride concentrations were not increased with increasing heads in the boundary conditions in either the rivers or Delaware Bay to more easily identify the mechanisms increasing the total mass within the aquifer. However, higher concentrations would be expected in reality as the salt front in the rivers moves further inland with SLR (Bhuiyan & Dutta, 2012; DRBC, 2019).

Although the process of salinization may refer to any increase in salinity, here we define "saline" as wells or cells with a concentration greater than or equal to 250 ppm of chloride, the secondary maximum contaminant level (SMCL) set by the U.S. Environmental Protection Agency and "salinized" as wells where the concentration increased to 250 ppm or above. Irrigating with water of 250 ppm of chloride may cause harm to plants depending on their salinity tolerance (Maas & Hoffman, 1977). Corn is the main crop grown in the study area and is moderately sensitive to salt, with a negative impact to yield seen at approximately 3.5% of seawater, which translates to 340 ppm chloride (Butcher et al., 2018).

3. Results

3.1. Comparison of the Model and AEM Survey

The AEM resistivity sections showed strongly electrically conductive (low resistivity) areas consistent with inland salinization of groundwater restricted to the area under the marsh, where the freshwater has pushed the deep part of the freshwater-saltwater interface away from the marsh-land intersection toward Delaware Bay, reversing the classic wedge-shape of the freshwater-saltwater interface. These findings are in agreement with our model results.

3.2. Current Pumping Rates and Sea-Level Rise

Pumping at current rates without SLR (Scenario *A*) leads to saline areas occurring primarily in cells adjacent to the marsh boundary and tidal streams at the center of the model domain (Figure 3a). After 100 years of pumping at current rates and without SLR, there was less than a 1% increase in the total freshwater volume (i.e., model cells that are not within or beneath the marsh or Delaware Bay area) that became saline (Table 3).

The areas of greatest increase in chloride concentration due to SLR are located around the tidal streams in the center of the model, not along the freshwater-saltwater interface below the marsh (Figure 3b), showing for our model the dominant pathway for salinization is surface water bodies instead of inland migration of the salt wedge. Moving forward, we refer to the freshwater-saltwater interface beneath the marsh, as shown in Figure 2, as the "main interface." Increases in chloride concentration within the main interface are limited to beneath the marsh area and would not immediately impact groundwater use inland (Figure 3). Comparing end-time chloride concentrations between the scenarios of current pumping rates with and without SLR, SLR would salinize 2% of the total freshwater volume to chloride concentrations above 250 ppm. This increase can be seen in Figure 3, located along the tidal streams. Similar to the case without SLR, the dominant pathway of salinization is from the streams, but the SLR-elevated heads in the streams results in higher fluxes of salt water into the aquifer from the streams.

3.3. Distributed Versus Concentrated Pumping and Compounding Effects From SLR

Increased pumping at widely distributed irrigation wells (Scenario *B*) resulted in salinization of a greater volume of freshwater compared to the equivalent increase in pumping rate at the more concentrated municipal wells. However, increased municipal pumping (Scenario *C*) caused more intensive salinization in a smaller area compared to the irrigation increase (Figures 4a, 4b, 4d, and 4e). The model cells that were impacted by increased irrigation pumping were located in the bottom layers of the southern half of the model beneath the marsh area near the second highest-pumping irrigation well. Most of these cells increased less than 50 ppm and did not have much effect on the main interface (Figure 4). Although both scenarios (B and C) increased chloride concentrations near tidal streams, the municipal pumping led to greater increases in chloride, notably in the top layer because the concentrated pumping enhances the head drawdown near the streams (Figures S2 and S3 in Supporting Information S1). At the end of the increased municipal pumping scenario, 21% of the original freshwater volume became saline. Increasing irrigation pumping caused 17% to become saline (Table 3).

Coupling SLR with increased pumping led to the highest levels of chloride in the model, but there were slight differences among each scenario. SLR combined with increased irrigation pumping led to a saline volume of 20%,

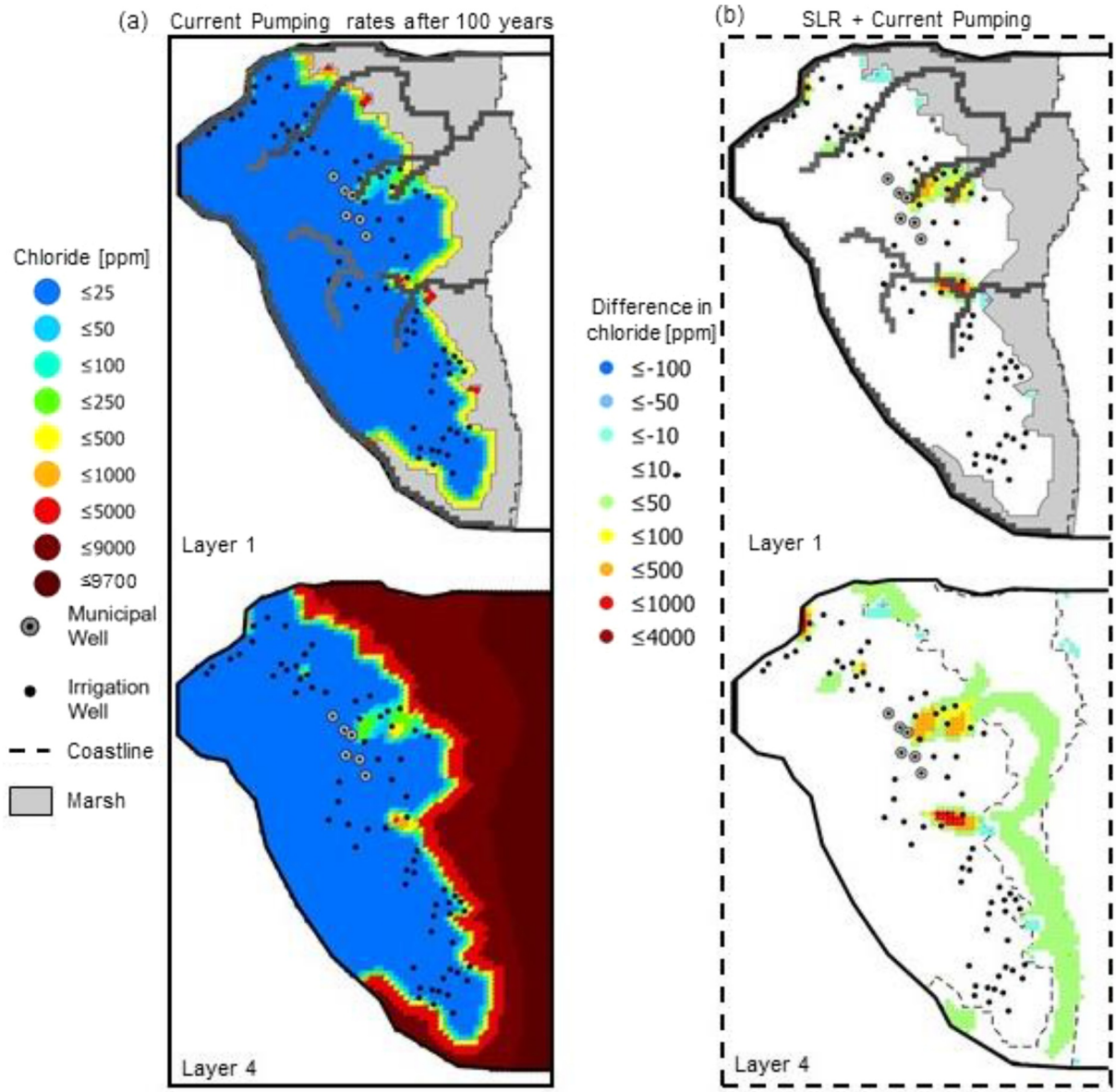

Figure 3. Model results for scenario A and A + SLR. (a) Distribution of chloride concentrations in the top and bottom layers in 100 years with current pumping rates and static sea level. (b) Difference in chloride concentrations between Scenario A + SLR and Scenario *A*, where negative numbers represent a decrease in concentration in Scenario A + SLR compared to Scenario (a) The gray area represents the marsh boundary condition in the top layer wherein the concentration is specified as 9,000 ppm for all scenarios. *Differences smaller than 10 ppm not shown.

compared to 25% with increased municipal pumping and SLR (Table 3). The inland extent of the 250-ppm contour along the edge of the marsh (i.e., where the main subsurface saltwater-freshwater interface would typically be monitored) remained largely unchanged by SLR or any of the scenarios, shifting less than 4 m (Figure 5). Changes in location of this contour can be seen around the tidal streams in the middle portion of the model.

Pumping the municipal wells at their maximum permitted rate (Scenario *D*) led to substantial increases in chloride around the tidal streams, along with increases in chloride along and beneath the marsh area in the middle of the model (Figures 4c and 4f). At this maximum rate, 34% of the original freshwater volume would be saline without SLR, and 36% would become saline with SLR (Table 3). Despite this high increase in pumping, the main interface beneath the marsh did not migrate further inland (Figure 5).

Table 3
Percent of Total Freshwater Volume (i.e., Total Number of Cells in the Model Excluding Cells In/Under the Marsh and Bay) at Different Chloride Concentrations for No Pumping (Steady State), Present Day, and for Each Scenario After 100 Years

			No sea-level rise				Sea-level rise			
Chloride concentration	No pumping (%)	Present day (%)	Current pumping rates (%)	Increased irrigation (%)	Increased municipal (%)	Max municipal (%)	Current pumping rates (%)	Increased irrigation (%)	Increased municipal (%)	Max municipal (%)
<250	87.5	84.8	84.8	83.1	79.3	66.3	81.6	79.9	75.3	64.4
250 – 500	9.8	11.4	11.4	12.2	13.3	14.2	12.7	13.2	14.4	14.5
500 – 1,000	0.9	1.8	1.8	2.2	4.2	7.7	2.4	2.9	4.7	7.9
1,000 – 5,000	1.8	2.0	2.0	2.4	3.2	11.9	3.3	4.0	5.5	13.3

3.4. Salinized Wells

Out of the 69 irrigation wells included in the model, 13 had ending (t = 100 years) chloride concentrations above 250 ppm for at least one of the scenarios. As shown in Figures 6 and 7, wells located in proximity to each other did not necessarily experience salinization in the same scenarios, and salinity levels varied. For instance, wells 5 and 6 are located 900 m apart, but well 5 was salinized in all scenarios whereas well 6 was salinized in four scenarios (Figures 6 and 7). The reduced frequency and degree of salinization of Well 6 can be attributed to its location on the other side of the tidal stream from Well 14, which is the largest-producing irrigation well (527 m^3/d). At the end of the current pumping rates scenario, three irrigation wells reached chloride concentrations greater than 250 ppm (Well 10: 292 ppm; Well 5: 297 ppm; Well 3: 305 ppm) (Figure 7). While most wells reached maximum chloride concentrations in the scenarios with maximum municipal pumping, Well 6 in the center of the model domain and Well 1 near the northern boundary reached peak chloride concentrations at the end of increased irrigation pumping with SLR scenario, and Well 7 had higher levels of chloride under increased municipal pumping compared to maximum municipal pumping. Seven irrigation wells had higher chloride levels from the increased municipal pumping scenarios than from the increased irrigation scenarios, both with and without SLR (Figure 7). Well 10, located in the southern part of the model domain, adjacent to the marsh, saw a decrease of approximately 25 ppm of chloride with both increased irrigation scenarios and almost no change in all the other scenarios.

Under current pumping rates, with or without SLR, the municipal wells remained near background concentrations (15 ppm) of chloride (Table 4). The municipal wells were largely unaffected by increased irrigation (i.e., <4 ppm change) even with SLR, but chloride concentrations increased in three of the six wells when municipal pumping was increased (Table 4). Wells *B* and *D* had minor increases, with ending concentrations between 40 and 50 ppm, and Well *C* increased to 143 ppm. Coupling SLR with increasing municipal pumping elevated these concentrations to 61 ppm (B), 86 ppm (D), and 207 ppm (C). When the municipal wells were pumped at their maximum rates, both with and without SLR, four (B, C, D, and F) of the six municipal wells experienced increases greater than 150 ppm, with three wells (B, C and D) having ending (t = 100 years) chloride concentrations above 250 ppm (Table 4).

Of the approximately 300 domestic wells located within the model area with a completion depth of <16 m, two had simulated concentrations exceeding 250 ppm chloride at current pumping rates in 100 years (Figure 5). Increasing irrigation would salinize eight domestic wells, and increasing municipal pumping would salinize 10 (Figure 5). If the municipal wells were to pump at their maximum permitted limits, 15 domestic wells would be above the SMCL for chloride. Sea-level rise would salinize 11 domestic wells when coupled with current pumping rates, increased irrigation, or increased municipal pumping; however, pumping the municipal wells at the maximum rates with 1 m of SLR would salinize 21 domestic wells.

3.5. Sources and Sinks

River boundary conditions were the main source of chloride entering the aquifer during the scenarios, not the constant head boundary. The largest differences in mass coming into the aquifer among scenarios came from the river boundary conditions (Figure 8a). Although total percentage of mass from river leakage into the model was less than 2% for all the scenarios, noticeable changes in the rate of river leakage into the model can be seen in Figure 8b. Changes in river leakage into the model from increased pumping began to level off after 10 years, indicating that changes in water levels adjust relatively quickly to pumping (Figure 8b). As SLR was applied

10.1029/2023WR035840

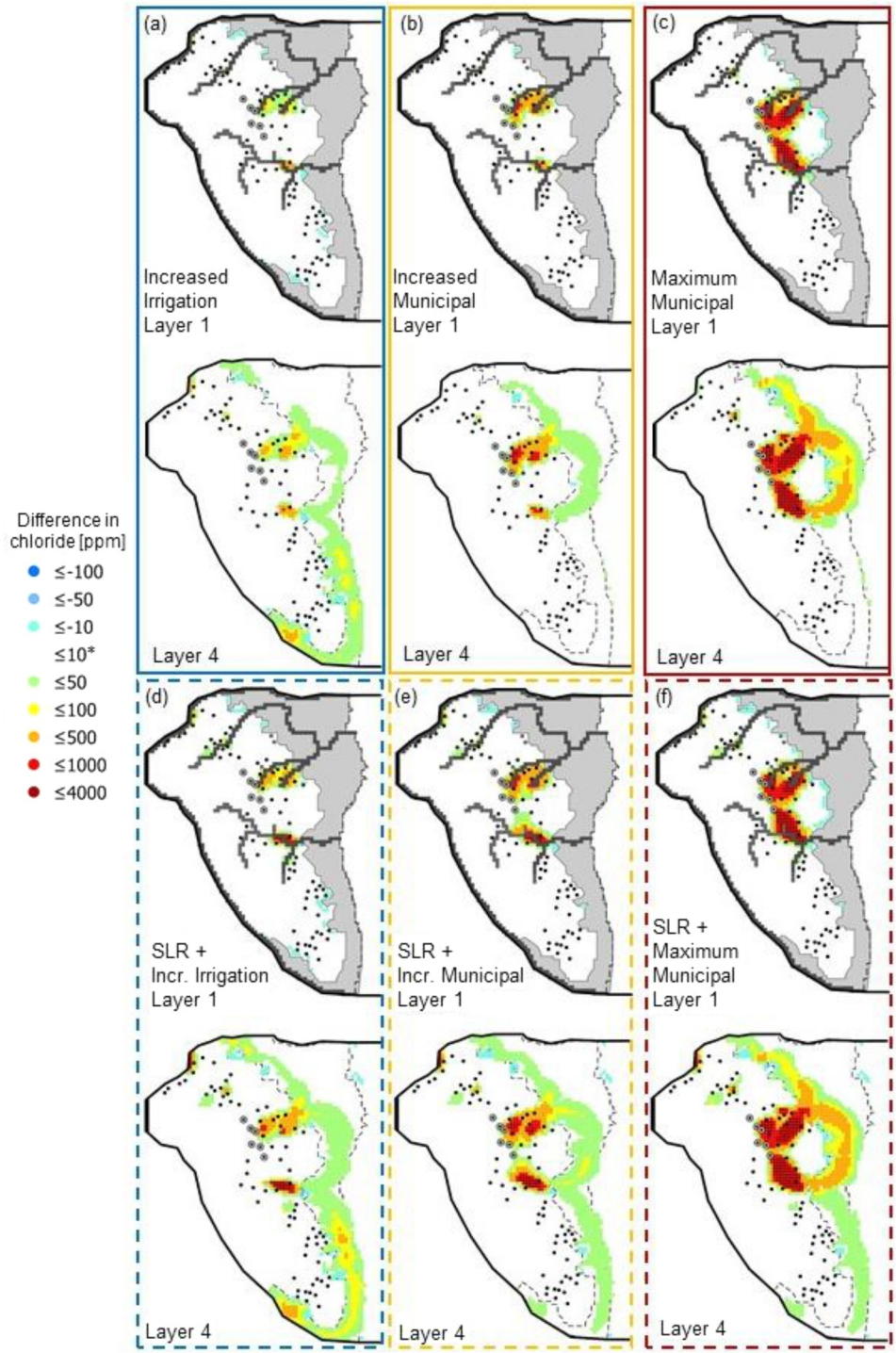

Figure 4. Differences in chloride concentrations between noted scenario and current pumping rates after 100 years. (a) Scenario *B* increased irrigation pumping. (b) Scenario *C* increased municipal pumping. (c) Scenario *D* maximum municipal pumping. (d) Scenario B + SLR. (e) Scenario C + SLR. (f) Scenario D + SLR. Negative numbers indicate a decrease in concentration. *Differences less than 10 ppm not shown.

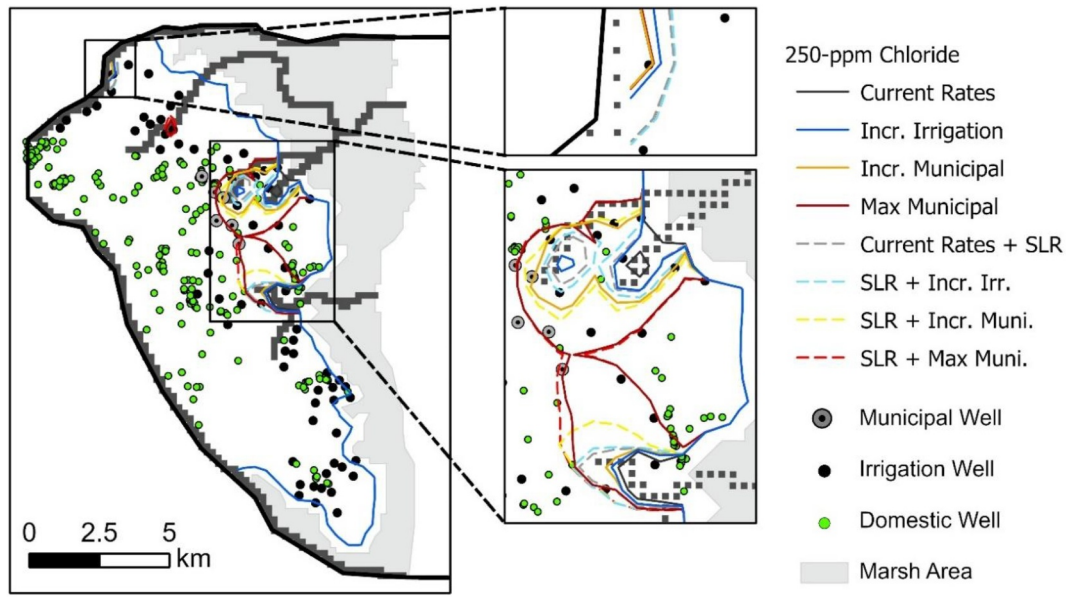

Figure 5. Location of the 250-ppm contour in Layer 4. Domestic wells (green circles) which were not included in the model are shown to highlight impact to drinking water.

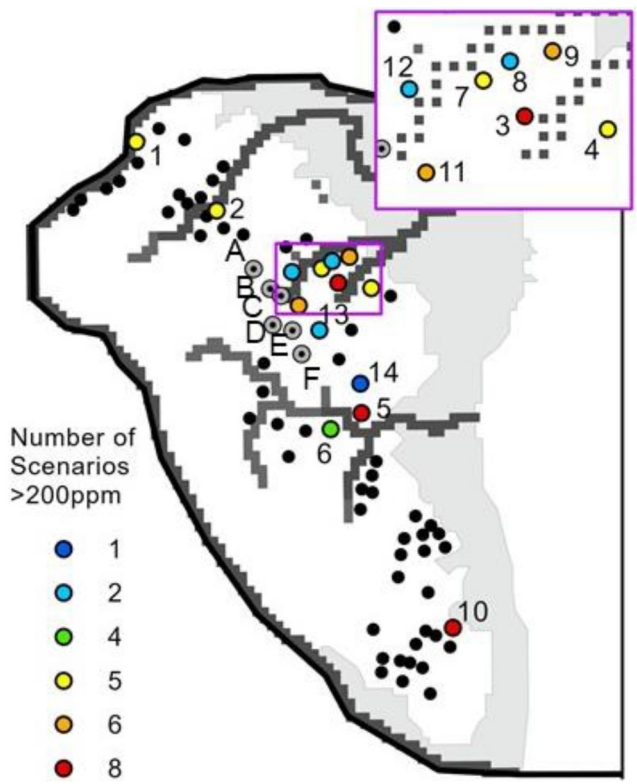

Figure 6. Map showing irrigation wells (number is well ID) that had a chloride concentration above 200 ppm in at least one scenario. Gray circles with black centers are municipal wells and are labeled with a letter (A–F).

gradually throughout the duration of scenarios, river leakage rates also continued to increase steadily throughout the scenarios with SLR.

4. Discussion

4.1. Importance of Surface Water-Groundwater Connections

Traditionally SWI studies assume the coastline acts as a defined, linear boundary between fresh and saline water. Our study highlights how the coastline is not always so clear-cut and that tidal streams and marshlands considerably complicate characterizing risk of SWI due to both pumping and SLR. The low permeability of marsh sediments limits vertical infiltration of saltwater and inverts the typical freshwater-saltwater wedge, by allowing freshwater to flow beneath saltwater (Figure 2). There were only minor increases (<50 ppm) in chloride concentrations along the marsh edge in all scenarios (Figures 3b and 4). Saltmarshes have been previously shown to buffer developed land against surface inundation driven by SLR and storm surges (Guimond & Michael, 2021), and current results indicate that marshes may buffer groundwater from SWI by not allowing the saltwater to infiltrate as quickly compared to arable land.

If saline tidal streams had not been included in our model, and we only assessed the migration of the main transition zone, we would have concluded that this area is not at substantial risk for SWI. As demonstrated in our results, there is high risk of salinization to wells located near tidal streams, farther inland than the main transition zone (Figures 3 and 5). Tidal streams act as local extensions of the sea and thus can act as sources of saltwater, and therefore need to be included in modeling studies to assess the full risk of salinization. Under typical conditions, these streams are net gaining, with minor periods of possible losing conditions tidally or seasonally. However, once the hydraulic gradient shifts the stream from net-gaining to net-losing due to pumping, SLR, or both, the saline part of the stream becomes a source of salt to the aquifer. Salt-fronts in large rivers from which

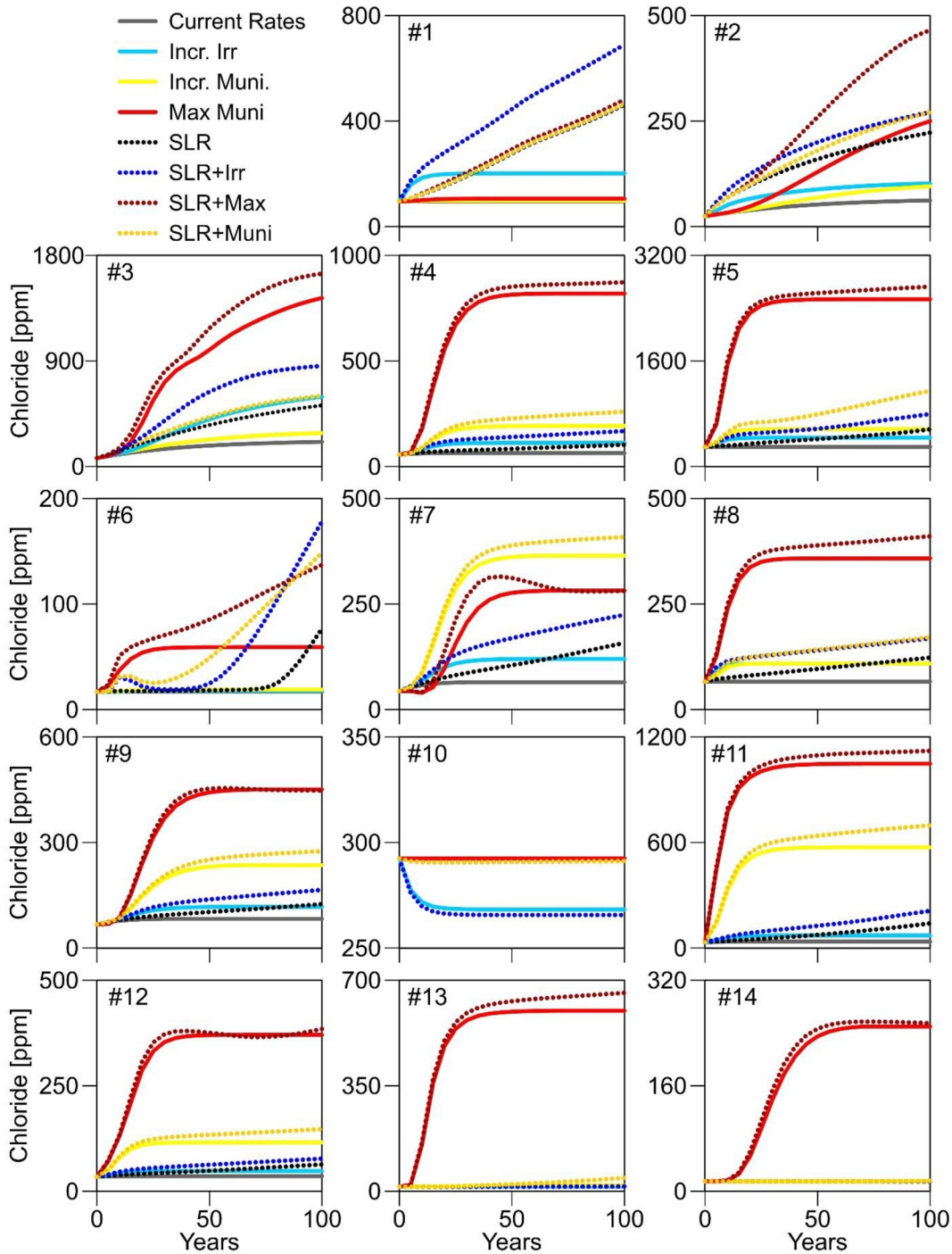

Figure 7. Time series plots of irrigation wells with chloride concentrations above 250 ppm for at least one scenario.

municipalities withdraw water are often monitored (e.g., Delaware River Basin Commission) but monitoring in smaller streams that do not serve as direct water sources is rare. In areas of heavy groundwater use, these smaller tidal streams could lead to extensive aquifer salinization if in proximity to pumping wells. As shown in Figure 8, the greatest difference in salt mass into the aquifer between scenarios came from river boundary conditions, because recharge volume is constant for all scenarios. Since river boundaries were applied to only the top layer, chloride initially entered the top of the model and then migrated vertically downward (Figure S4 in Supporting Information S1). Figure 8b highlights how increases in pumping and SLR increase the mass coming in from

Table 4
Chloride Concentrations in Municipal Wells (Locations Shown on Figure 6) After 100 Years of Each Scenario

Scenario	A	B	C	D	E	F
Current rates	15	15	17	15	15	15
Incr. Irrigation	15	15	18	15	15	15
Inc. Municipal	15	41	143	15	50	16
Max municipal	15	**295**	**597**	18	**382**	171
SLR + Current rates	15	15	20.	15	17	15
SLR + Incr. Irrigation	15	15	21	15	17	15
SLR + Incr. Municipal	15	61	207	16	86	21
SLR + Max muni.	15	**343**	**611**	18	**420**	232

Note. Bold indicates exceedance of the 250 ppm EPA SMCL.

rivers, primarily from the two rivers in the middle of the model, where adjacent cells experienced the greatest increases in chloride (Figures 3b and 4). This model uses long-term averages of water levels and chloride concentrations for boundary conditions to assess general trends. It does not account for short-term fluctuations, such as tides which induce continuously varying heads and salinity levels in coastal streams which would affect whether the stream is gaining or losing, and how much saltwater is entering the aquifer. Even if streams are gaining, saltwater can still enter the aquifer due to density differences between the fresh groundwater and saline stream water as demonstrated by Werner and Lockington (2006). While they found that tides did significantly impact the amount of salt entering the aquifer, even at steady-state (no tidal fluctuation) a salt plume developed in the surrounding aquifer (Werner & Lockington, 2006).

4.2. Spatial Distribution of Pumping

Areas of highly concentrated pumping, such as the Dover municipal wells, could disproportionately and unintentionally impact smaller individual users. In our increased irrigation and municipal pumping scenarios, the total extraction rate was the same, but increasing the municipal pumping rates resulted in more intensive salinization and a greater number of salinized irrigation and domestic wells compared to increasing irrigation pumping rates (Figure 5). Municipalities are likely to have wells clustered near each other due to limited land availability and cost of infrastructure, such as pipelines. Irrigation wells 1 and 2 did experience large increases in chloride with increased irrigation pumping (Figure 5). Both wells are located along streams in the northern half of the model and are in proximity (<1,000 m) to a much larger-producing well (>260 m^3/d). These wells (1 and 2), along with the results from increasing municipal pumping indicate that salinity in some wells may be affected by larger-producing wells and efforts made by the more vulnerable well owners take to mitigate SWI may not be enough to counter the impact from the larger wells. The area of influence of such larger wells will depend on their pumping rate and the hydrogeologic properties of the aquifer. Many studies have looked at determining the optimal pumping rates of wells in a system that will limit salinization while maximizing production, but these studies fail to consider the independent agency of water users, particularly irrigators, who likely make decisions based on their own need and do not consider the impacts to other water users (e.g., Cheng et al., 2000; Dhar & Datta, 2009; Mantoglou, 2003). There is a need to understand how water-users' behaviors may be altered if they are educated about how their personal decisions can negatively impact other users. When conducting feasibility studies for new, large production wells, the impact to the entire hydrologic system should be considered instead of basing citing and design only on well performance.

4.3. Competing Water Users

As availability of freshwater resources becomes limited due to climate change and overuse, there is increasing competition among water users. This is especially true in areas like the western United States, where unreliable precipitation rates are creating competition for groundwater between cities with growing populations and farmers who need to irrigate their crops (Konikow & Kendy, 2005; Liu et al., 2022). Historically, the East Coast of the United States has not had issues with limited groundwater supplies like that of the West Coast. However, SWI intrusion may increase the risk of salinization to freshwater and lead to the need for more stringent water use limitations. In the State of Delaware, irrigators who use more than 50,000 gallons per day are required to have a water permit and a withdrawal limit is assigned with expectations that the irrigator will report accurate usage rates (DNREC Water Supply Assessment and Protection (WSAP) program). However, while developing this model, we found most permitted wells lacked reported usage rates which limits the accuracy of this or any future model. Additionally, permitted extraction rates are based on small-scale models for each well that do not account for all wells in the entire region. Dover does have permit limits which restrict use to 3 million gallons per day combined for the wells completed in the Columbia aquifer (WR & A, 2021). As previously shown by He and Andres (2018), pumping at this rate would result in the severe decline in water levels, and our model shows that pumping at such rates could result in intense and extensive salinization of the aquifer. A review of the 2021 Dover Water Master Plan indicated that maximum pumping rates are limited by the pumps and capacity of the water treatment plant but makes no mention of the hydrogeologic limitations of the aquifer (WR & A 2021). The city of Dover is likely

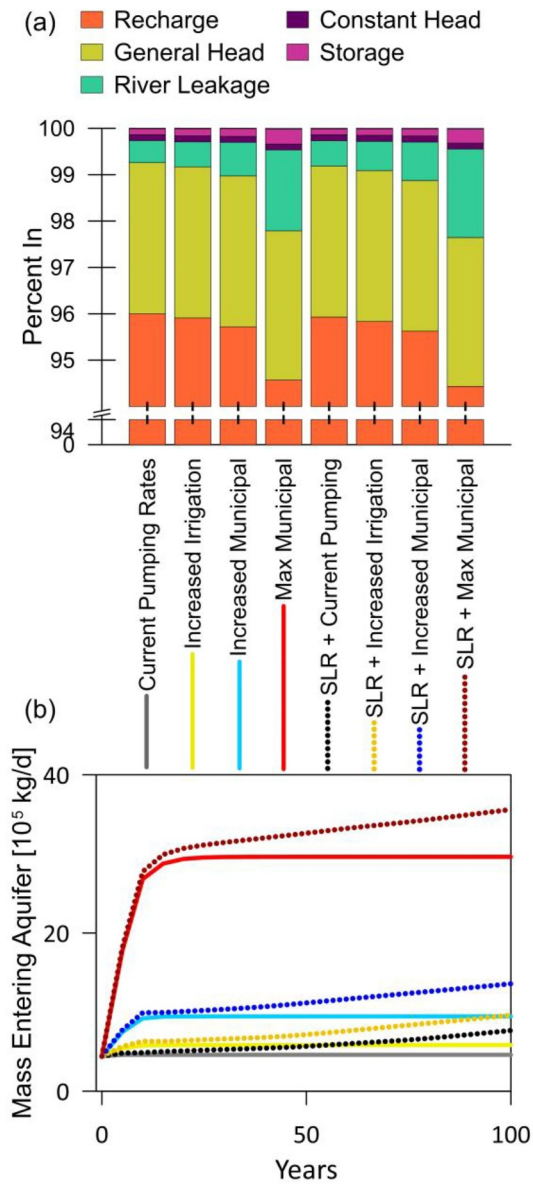

Figure 8. (a) Percent of total mass coming into the aquifer from the boundary conditions. (b) Rate of total mass entering the aquifer from river leakage.

not unique in its approach when assessing new permits. In the United States, for example, historically water rights and allocations have focused mainly on surface water sources while groundwater usage has gone largely unregulated in comparison (Kirchhoff & Dilling, 2016). With increased interest in utilizing groundwater sources that are less susceptible to impacts from short-term drought conditions relative to surface water sources, accurate usage monitoring and groundwater models could provide water managers with better estimates of sustainable extraction rates.

4.4. Economic Implications

When conducting scientific research on water resources, it is important to frame changes in the hydrologic system in terms of economics as that is often the driving factor for resource managers and policy makers. Assuming that SLR is inevitable, the scenarios that included SLR could be the most likely to occur. We found that 13 to 14 irrigation wells would become salinized, which equates to around 20% of all irrigation wells within the model.

Though irrigation water of 250 ppm may not kill entire crops, salts could accumulate in the soils and begin to stress plants. The farms represented by the salinized wells vary in area from 10 to 160 acres. The USDA estimated that the net profit in 2021 in Delaware from 1 acre of corn was $490.78 (USDA NASS). Even a 10% reduction in crop production could have meaningful impacts on farmers' profits, causing annual losses up to $7,852 for an individual farmer. While these amounts are Delaware-specific, the prevalence of agriculture in coastal areas around the world means there is substantial economic risk from SWI. Kummu et al. (2016) estimated that coastal zones produce approximately 42% of the global gross domestic product, with agricultural operations contributing a large portion of that amount. Additionally, salinizing domestic wells could cause homeowners to lose their supply of clean drinking water, forcing them to invest in filtration systems, relocate, or have the city expand their municipal supply lines.

4.5. Model Limitations

While our model is more hydrologically complex than many other SWI models with the inclusion of tidal streams and marshes, there remain dynamics of coastal hydrology that we could not capture in a single model of this scale. In this study, we simulate SLR as a steady increase in heads only, while in reality, sea level is constantly fluctuating due to tides and seasonal thermal expansion. We also did not increase chloride levels in the boundary conditions of which we increased heads for SLR. SLR is expected to increase salinity levels in the Delaware Bay which would also increase salinity levels and extent in tidal streams, which would be expected to result in even greater salinization of the study area. As the purpose of this study was to assess long-term changes in the system, we used average annual values for recharge, pumping and river boundary conditions. We did not assess short-term fluctuations in salinization that may occur due to temporally varying tides and the intermittency of irrigation pumping, such as pumping at high tide versus low tide, or how storm surges may cause a regime shift in current salinity distribution. Like many other groundwater models, we assigned a homogenous hydraulic conductivity value to the area of developed land and applied a uniform thickness, though, the Columbia aquifer has been found to be heterogeneous in conductivity and thickness. Inclusion of localized confining muddy beds that have been found within the Columbia aquifer may alter salinization patterns (Hingst et al., 2022). The results of the AEM survey can be used to interpret heterogeneity of sediments and salinity distributions for incorporation to the existing SWI model. Additionally, because rivers and streams were shown to be dominant pathways of salinization, their boundary condition values could have a substantial impact on the degree and extent of salinization. Future SWI studies could collect more field data on the hydraulic properties of riverbeds to better constrain the boundary conditions in corresponding models.

5. Conclusions

Saltwater intrusion has been extensively studied and modeled both in hypothetical situations and for site specific cases. However, these studies often fail to assess the impacts surface water-groundwater connections could have on groundwater salinization. Specifically, there is a lack of SWI studies which include tidal marshes and streams as possible sources of salinization. Here we constructed a model to determine what impact salty tidal streams and marshland could have on the extent of salinization in a coastal area that is subject to SLR and has competing water users. We found that the presence of the marsh inverted the freshwater-saltwater interface expected from a typical coastal beach boundary, and this inversion is supported by the resistivity structure observed from a recent AEM survey of the model area. Salinization was greatest around tidal streams in the center of the model. Wells located next to these streams experienced greater salinization than wells located closer to the marsh and coastline. These results demonstrate that in coastlines where pumping and tidal streams are spatially coincident, entrainment of saline water from tidal streams into the aquifer can occur on a shorter timescale and over a broader area than salinization driven by the inland migration of the saltwater wedge. Groundwater pumping in proximity to tidal streams is prevalent globally, and as SLR continues, there will be an increase in the level of salinity and inland extent of saline water in tidal streams. Therefore, the dominance of salinization from tidal streams in areas of pumping highlights the potential importance of this pathway as a mechanism for salinization globally. We also found that the spatial distribution of pumping matters, especially as it is related to competing water users, because an increase in pumping concentrated in the center of the model caused more intensive salinization than an equal but more widely distributed increase in pumping. While our model incorporates more hydrological complexity than many other SWI models by including tidal streams and marshes as sources of salinity and pumping wells, it still does not capture all coastal hydrology dynamics, such as tides and the resulting fluctuating salinity. Future

models could assess the salinity dynamics in aquifers due to coupled tidal fluctuations and intermittent pumping. When assessing the risk of SWI to groundwater in a coastal environment, it is imperative to include surface water bodies, especially if tidally influenced, in order to construct an accurate representation of the hydrologic system. Not including surface-water and groundwater interactions could result in underestimation of risk of salinization which has been shown to have negative economic impacts.

Data Availability Statement

Modeling input files are publicly available from CUAHSI Hydroshare (Hingst, 2024). AEM survey data are available from U.S. Geological Survey (2024).

Acknowledgments
This project was conducted as part of Project WiCCED (Water in the Changing Coastal Environment of Delaware), which is funded by the National Science Foundation EPSCoR Grant OIA1757353 and the State of Delaware. Funding for MH was also obtained from the Delaware Environmental Institute. Any use of trade, firm, or product names is for descriptive purposes only and does not imply endorsement by the U.S. Government. Support for the geophysical survey and data analysis was provided by the USGS Delaware River Basin Next Generation Water Observing System (NGWOS) project.

References

Abd-Elhamid, H. F., Abd-Elaty, I., & Sherif, M. M. (2019). Effects of aquifer bed slope and sea level on saltwater intrusion in coastal aquifers. *Hydrology*, *7*(1), 5. https://doi.org/10.3390/hydrology7010005

Airborne Topographic LiDAR Report Sandy Delaware & Maryland. (2015). Quantum spatial. Retrieved from https://enterprise.firstmap.delaware.gov/arcgis/rest/services/Elevation

Andres, A. (2004). *Groundwater recharge potential mapping in Kent and Sussex counties, Delaware (Report of investigations No. 66.)*. Delaware Geological Survey.

Andres, A. S., & Klingbeil, A. D. (2006). *Thickness and transmissivity of the unconfined aquifer of Eastern Sussex county, Delaware (report of investigations No. 70)*. Delaware Geological Survey.

Andres, A. S., McQuiggan, R. W., He, C., & McKenna, T. E. (2023). *Kent county groundwater-monitoring project: Results of hydrogeological studies (report of investigations 85)*. Delaware Geological Survey.

Andres, A. S., McQuiggan, R. W., He, C., & Wunsch, D. R. (2019). *Kent County groundwater monitoring project: Results of subsurface exploration state of Delaware (Open File Report No. 53)*. Delaware Geological Survey.

Archie, G. E. (1947). Electrical resistivity an aid in core-analysis interpretation. *AAPG Bulletin*, *31*(2), 350–366. https://doi.org/10.1306/3D93395C-16B1-11D7-8645000102C1865D

Ator, S. W., Denver, J. M., Krantz, D. E., Newell, W. L., & Martucci, S. K. (2005). *A surficial Hydrogeologic framework for the Mid-Atlantic Coastal Plain* (Vol. 1680). US Department of the Interior, US Geological Survey. https://doi.org/10.3133/pp1680

Back, W., & Freeze, R. A. (1983). *Physical hydrogeology*. Hutchinson Ross Publishing Company.

Bakker, M. (2003). A Dupuit formulation for modeling seawater intrusion in regional aquifer systems. *Water Resources Research*, *39*(5), 1131. https://doi.org/10.1029/2002WR001710

Barlow, P. M., & Reichard, E. G. (2010). Saltwater intrusion in coastal regions of North America. *Hydrogeology Journal*, *18*(1), 247–260. https://doi.org/10.1007/s10040-009-0514-3

Bhuiyan, M. J. A. N., & Dutta, D. (2012). Assessing impacts of sea level rise on river salinity in the Gorai river network, Bangladesh. *Estuarine, Coastal and Shelf Science*, *96*, 219–227. https://doi.org/10.1016/j.ecss.2011.11.005

Bobba, A. G. (1993). Mathematical models for saltwater intrusion in coastal aquifers. *Water Resources Management*, *7*(1), 3–37. https://doi.org/10.1007/BF00872240

Brinson, K. (2023). *Exploring Hydroclimatic variability for agricultural and water resource applications on the Delmarva peninsula, (doctoral dissertation)*. University of Delaware.

Brunner, P., Simmons, C. T., Cook, P. G., & Therrien, R. (2010). Modeling surface water-groundwater interaction with MODFLOW: Some considerations. *Ground Water*, *48*(2), 174–180. https://doi.org/10.1111/j.1745-6584.2009.00644.x

Butcher, K., Wick, A. F., DeSutter, T., Chatterjee, A., & Harmon, J. (2018). Corn and soybean yield response to salinity influenced by soil texture. *Agronomy Journal*, *110*(4), 1243–1253. https://doi.org/10.2134/agronj2017.10.0619

Calver, A. (2001). Riverbed permeabilities: Information from pooled data. *Ground Water*, *39*(4), 546–553. https://doi.org/10.1111/j.1745-6584.2001.tb02343.x

Carr, P. A. (1969). Salt-water intrusion in prince Edward Island. *Canadian Journal of Earth Sciences*, *6*(1), 63–74. https://doi.org/10.1139/e69-007

Chang, S. W., & Clement, T. P. (2012). Experimental and numerical investigation of saltwater intrusion dynamics in flux-controlled groundwater systems. *Water Resources Research*, *48*(9), W09527. https://doi.org/10.1029/2012WR012134

Cheng, A. D., Halhal, D., Naji, A., & Ouazar, D. (2000). Pumping optimization in saltwater-intruded coastal aquifers. *Water Resources Research*, *36*(8), 2155–2165. https://doi.org/10.1029/2000WR900149

Cook, S. E., Warner, J. C., & Russell, K. L. (2023). A numerical investigation of the mechanisms controlling salt intrusion in the Delaware Bay estuary. *Estuarine, Coastal and Shelf Science*, *283*, 108257. https://doi.org/10.1016/j.ecss.2023.108257

Costa, Y., Martins, I., de Carvalho, G. C., & Barros, F. (2023). Trends of sea-level rise effects on estuaries and estimates of future saline intrusion. *Ocean & Coastal Management*, *236*, 106490. https://doi.org/10.1016/j.ocecoaman.2023.106490

Delaware Climate Office. (n.d.). *1981–2010 Delaware climate normals*. University of Delaware Center for Envrionmental Monitoring. Data from the Dover station. Retrieved from http://pegasus.cema.udel.edu/applications/CLIMATE_NORM_WEB_PAGE/

Delaware Coastal Inundation Map. (2017). Delaware geological survey. Retrieved from https://enterprise.firstmap.delaware.gov/arcgis/rest/services/Environmental/DE_Coastal_Inundation_2017/MapServer

Delaware Coastal Programs of the Department of Natural Resources and Environmental Control. (2012). Preparing for tomorrow's high tide: Sea level rise vulnerability assessment for the state of Delaware. In *Prepared for the Delaware Sea Level advisory committee*. Retrieved from http://de.gov/slradvisorycommittee/

Delaware Department of Natural Resources and Environmental Control (DNREC). (2012). Water Supply Assessment and Protection (WSAP) program. Retrieved from https://dnrec.delaware.gov/water/commercial-government/water-allocation/

Delaware River Basin Commission. (2019). State of the Delaware River Basin 2019. Retrieved from https://www.nj.gov/drbc/public/publications/SOTB2019.html

Dhar, A., & Datta, B. (2009). Saltwater intrusion management of coastal aquifers. I: Linked simulation-optimization. *Journal of Hydrologic Engineering*, *14*(12), 1263–1272. https://doi.org/10.1061/(ASCE)HE.1943-5584.0000097

ESRI. (2009). World imagery Basemap. *ArcGIS Pro*.
Fenstermacher, D. E., Rabenhorst, M. C., Lang, M. W., McCarty, G. W., & Needelman, B. A. (2014). Distribution, morphometry, and land use of Delmarva Bays. *Wetlands*, *34*(6), 1219–1228. https://doi.org/10.1007/s13157-014-0583-5
Fitterman, D. V., & Deszcz-Pan, M. (1998). Helicopter EM mapping of saltwater intrusion in Everglades national park, Florida. *Exploration Geophysics*, *29*(1–2), 240–243. https://doi.org/10.1071/EG998240
Galperin, B., & Mellor, G. L. (1990). Salinity intrusion and residual circulation in Delaware Bay during the drought of 1984. *Residual Currents and Long-Term Transport*, *38*, 469–480. https://doi.org/10.1029/CE038p0469
Goswami, R. R., & Clement, T. P. (2007). Laboratory-scale investigation of saltwater intrusion dynamics. *Water Resources Research*, *43*(4). https://doi.org/10.1029/2006WR005151
Guimond, J., & Tamborski, J. (2021). Salt marsh hydrogeology: A review. *Water*, *13*(4), 543. https://doi.org/10.3390/w13040543
Guimond, J. A., & Michael, H. A. (2021). Effects of marsh migration on flooding, saltwater intrusion, and crop yield in coastal agricultural land subject to storm surge inundation. *Water Resources Research*, *57*(2), e2020WR028326. https://doi.org/10.1029/2020WR028326
Guimond, J. A., Seyfferth, A. L., Moffett, K. B., & Michael, H. A. (2020). A physical-biogeochemical mechanism for negative feedback between marsh crabs and carbon storage. *Environmental Research Letters*, *15*(3), 034024. https://doi.org/10.1088/1748-9326/ab60e2
Guo, W., & Langevin, C. D. (2002). User's guide to SEAWAT; a computer program for simulation of three-dimensional variable-density ground-water flow. *Techniques of water-resources investigations, (06-A7)*.
Han, D., & Currell, M. J. (2022). Review of drivers and threats to coastal groundwater quality in China. *Science of the Total Environment*, *806*, 150913. https://doi.org/10.1016/j.scitotenv.2021.150913
He, C., & Andres, A. S. (2018). *Results of groundwater flow simulations in the east dover area, Delaware (open file report. 52.)*. Delaware Geological Survey.
Hingst, M. (2024). East_Dover_SEAWAT_Model_VisualModflowFlex, HydroShare [model files]. http://www.hydroshare.org/resource/2aff1c01284445e08b6ed4b1a71bb3bb
Hingst, M. C., McQuiggan, R. W., Peters, C. N., He, C., Andres, A. S., & Michael, H. A. (2022). Surface water-groundwater connections as pathways for inland salinization of coastal aquifers. *Ground Water*, *61*(5), 626–638. https://doi.org/10.1111/gwat.13274
Kalbus, E., Reinstorf, F., & Schirmer, M. (2006). Measuring methods for groundwater–surface water interactions: A review. *Hydrology and Earth System Sciences*, *10*(6), 873–887. https://doi.org/10.5194/hess-10-873-2006
Kazakis, N., Busico, G., Colombani, N., Mastrocicco, M., Pavlou, A., & Voudouris, K. (2019). GALDIT-SUSI a modified method to account for surface water bodies in the assessment of aquifer vulnerability to seawater intrusion. *Journal of Environmental Management*, *235*, 257–265. https://doi.org/10.1016/j.jenvman.2019.01.069
Kidwell, S. M. (1984). *Outcrop features and origin of basin margin unconformities in the lower Chesapeake Group (Miocene)*. Atlantic Coastal Plain.
Kirchhoff, C. J., & Dilling, L. (2016). The role of US states in facilitating effective water governance under stress and change. *Water Resources Research*, *52*(4), 2951–2964. https://doi.org/10.1002/2015WR018431
Kohout, F. A. (1960). Cyclic flow of salt water in the Biscayne aquifer of southeastern Florida. *Journal of Geophysical Research*, *65*(7), 2133–2141. https://doi.org/10.1029/JZ065i007p02133
Konikow, L. F., & Kendy, E. (2005). Groundwater depletion: A global problem. *Hydrogeology Journal*, *13*(1), 317–320. https://doi.org/10.1007/s10040-004-0411-8
Kummu, M., De Moel, H., Salvucci, G., Viviroli, D., Ward, P. J., & Varis, O. (2016). Over the hills and further away from coast: Global geospatial patterns of human and environment over the 20th–21st centuries. *Environmental Research Letters*, *11*(3), 034010. https://doi.org/10.1088/1748-9326/11/3/034010
Langevin, C. D., Thorne, D. T., Jr., Dausman, A. M., Sukop, M. C., & Guo, W. (2008). SEAWAT version 4: A computer program for simulation of multi-species solute and heat transport. *Techniques and methods*, 6–A22.
Lenkopane, M., Werner, A. D., Lockington, D. A., & Li, L. (2009). Influence of variable salinity conditions in a tidal creek on riparian groundwater flow and salinity dynamics. *Journal of Hydrology*, *375*(3–4), 536–545. https://doi.org/10.1016/j.ecss.2011.05.018
Liu, Y., Lin, Y., Huo, Z., Zhang, C., Wang, C., Xue, J., & Huang, G. (2022). Spatio-temporal variation of irrigation water requirements for wheat and maize in the Yellow River Basin, China, 1974–2017. *Agricultural Water Management*, *262*, 107451. https://doi.org/10.1016/j.agwat.2021.107451
Maas, E. V., & Hoffman, G. J. (1977). Crop salt tolerance—Current assessment. *Journal of the Irrigation and Drainage Division*, *103*(2), 115–134. https://doi.org/10.1061/JRCEA4.0001137
Mantoglou, A. (2003). Pumping management of coastal aquifers using analytical models of saltwater intrusion. *Water Resources Research*, *39*(12), 1335. https://doi.org/10.1029/2002WR001891
Martin, M. J., & Andres, A. S. (2008). *Analysis and summary of water-table maps for the Delaware Coastal Plain (report of investigations No. 73)*. Delaware Geological Survey.
Masterson, J. P., & Garabedian, S. P. (2007). Effects of sea-level rise on ground water flow in a coastal aquifer system. *Ground Water*, *45*(2), 209–217. https://doi.org/10.1111/j.1745-6584.2006.00279.x
McLaughlin, P. P., Tomlinson, J. L., & Lawson, A. K. (2009). *Aquifers and groundwater withdrawals, Kent and Sussex counties, Delaware (project contract report prepared for Delaware department of natural resources and environmental Control)*. Delaware Geological Survey.
Mclaughlin, P. P., & Velez, C. C. (2006). *Geology and extent of the confined aquifers of Kent County, Delaware by geology and extent of the confined aquifers of Kent County, Delaware (Report of Investigations No. 72)*. Delaware Geological Survey.
McOwen, C. J., Weatherdon, L. V., Van Bochove, J. W., Sullivan, E., Blyth, S., Zockler, C., et al. (2017). A global map of saltmarshes. *Biodiversity Data Journal*, *5*(5), e11764. https://doi.org/10.3897/BDJ.5.e11764
Meyer, R., Engesgaard, P., & Sonnenborg, T. O. (2019). Origin and dynamics of saltwater intrusion in a regional aquifer: Combining 3-D saltwater modeling with geophysical and geochemical data. *Water Resources Research*, *55*(3), 1792–1813. https://doi.org/10.1029/2018WR023624
Michot, B., Meselhe, E. A., Rivera-Monroy, V. H., Coronado-Molina, C., & Twilley, R. R. (2011). A tidal creek water budget: Estimation of groundwater discharge and overland flow using hydrologic modeling in the Southern Everglades. *Estuarine, Coastal and Shelf Science*, *93*(4), 438–448. https://doi.org/10.1016/j.ecss.2011.05.018
Miller, K. G., Kopp, R. E., Horton, B. P., Browning, J. V., & Kemp, A. C. (2013). A geological perspective on sea-level rise and its impacts along the US mid-Atlantic coast. *Earth's Future*, *1*(1), 3–18. https://doi.org/10.1002/2013EF000135
Moulds, M., Gould, I., Wright, I., Webster, D., & Magnone, D. (2023). Use of electrical resistivity tomography to reveal the shallow freshwater–saline interface in the Fens coastal groundwater, Eastern England (UK). *Hydrogeology Journal*, *31*(2), 335–349. https://doi.org/10.1007/s10040-022-02586-2

National Estuarine Research Reserve System (NERRS). (2003). System-wide monitoring program. *Data Accessed from the NOAA NERRS Centralized Data Management Office Website*, 1–32. https://doi.org/10.1201/9780203495605.ch1

Nield, S. P., Townley, L. R., & Barr, A. D. (1994). A framework for quantitative analysis of surface water-groundwater interaction: Flow geometry in a vertical section. *Water Resources Research*, *30*(8), 2461–2475. https://doi.org/10.1029/94WR00796

NOAA (National Oceanic and Atmospheric Administration). (n.d.). Delaware Bay OFS salinity Nowcast. Retrieved from https://tidesandcurrents.noaa.gov/ofs/ofs_mapplots.html?ofsregion=db&subdomain=0&model_type=salinity_nowcast

Olsson, R. K., Gibson, T. G., Hansen, H. J., & Owens, J. P. (1988). Geology of the Northern Atlantic Coastal Plain: Long island to Virginia.

Peters, C. N., Kimsal, C., Frederiks, R. S., Paldor, A., McQuiggan, R., & Michael, H. A. (2022). Groundwater pumping causes salinization of coastal streams due to baseflow depletion: Analytical framework and application to Savannah River, GA. *Journal of Hydrology*, *604*, 127238. https://doi.org/10.1016/j.jhydrol.2021.127238

Pinder, G. F., & Cooper, H. H., Jr. (1970). A numerical technique for calculating the transient position of the saltwater front. *Water Resources Research*, *6*(3), 875–882. https://doi.org/10.1029/WR006i003p00875

Raats, P. A. (2015). Salinity management in the coastal region of The Netherlands: A historical perspective. *Agricultural Water Management*, *157*, 12–30. https://doi.org/10.1016/j.agwat.2014.08.022

Rice, K. C., Hong, B., & Shen, J. (2012). Assessment of salinity intrusion in the James and Chickahominy rivers as a result of simulated sea-level rise in Chesapeake Bay, East Coast, USA. *Journal of Environmental Management*, *111*, 61–69. https://doi.org/10.1016/j.jenvman.2012.06.036

Richards, H. G. (1967). Stratigraphy of Atlantic Coastal Plain between long Island and Georgia. *AAPG Bulletin*, *51*(12), 2400–2429.

Sadeghi, S., Tootle, G., Elliott, E., Lakshmi, V., Therrell, M., & Kalra, A. (2019). Implications of the 2015–2016 El Niño on coastal Mississippi-Alabama streamflow and agriculture. *Hydrology*, *6*(4), 96. https://doi.org/10.3390/hydrology6040096

Setiawan, I., Morgan, L. K., & Doscher, C. (2023). Saltwater intrusion from an estuarine river: A field investigation. *Journal of Hydrology*, *617*, 128955. https://doi.org/10.1016/j.jhydrol.2022.128955

Shalem, Y., Yechieli, Y., Herut, B., & Weinstein, Y. (2019). Aquifer response to estuarine stream dynamics. *Water*, *11*(8), 1678. https://doi.org/10.3390/w11081678

Sophocleous, M. (2002). Interactions between groundwater and surface water: The state of the science. *Hydrogeology Journal*, *10*(1), 52–67. https://doi.org/10.1007/s10040-001-0170-8

Todd, D. K. (1953). Sea-water intrusion in coastal aquifers. *Eos, Transactions American Geophysical Union*, *34*(5), 749–754. https://doi.org/10.1029/TR034i005p00749

Tully, K., Gedan, K., Epanchin-Niell, R., Strong, A., Bernhardt, E. S., BenDor, T., et al. (2019). The invisible flood: The chemistry, ecology, and social implications of coastal saltwater intrusion. *BioScience*, *69*(5), 368–378. https://doi.org/10.1093/biosci/biz027

USDA NASS. (n.d.). United States department of agriculture national agricultural statistics service. Retrieved from https://quickstats.nass.usda.gov/

USGCRP. (2017). Climate science special report: Fourth national climate assessment. In V. I. Wuebbles, D. J. Fahey, K. A. Hibbard, D. J. Dokken, B. C. Stewart, et al. (Eds.), *U.S. Global change research program*. 470

U.S. Geological Survey. (2024). Airborne electromagnetic and magnetic survey of Delaware Bay and surrounding regions of New Jersey and Delaware, 2022: U.S. [Dataset]. *Geological Survey of Denmark Report*. https://doi.org/10.5066/F7J96592

Walther, M., Graf, T., Kolditz, O., Liedl, R., & Post, V. (2017). How significant is the slope of the sea-side boundary for modelling seawater intrusion in coastal aquifers? *Journal of Hydrology*, *551*, 648–659. https://doi.org/10.1016/j.jhydrol.2017.02.031

Waterloo Hydrogeologic. (2023). Visual MODFLOW Flex (version 8.0 | build 8.0.0.44343). [Software]. https://www.waterloohydrogeologic.com/visual-modflow-flex-8-0-product-release/

Werner, A. D., & Lockington, D. A. (2006). Tidal impacts on riparian salinities near estuaries. *Journal of Hydrology*, *328*(3–4), 511–522. https://doi.org/10.1016/j.jhydrol.2005.12.011

Whitman, Requardt & Associates LLP (WR&A). (2021). *Update to the water master Plan (contract No. 21-0013WW) final report*. City of Dover Delaware. Retrieved from https://www.cityofdover.com/departments/publicworks/UpdatetoWaterMasterPlanPresentation

Xiao, K., Li, H., Xia, Y., Yang, J., Wilson, A. M., Michael, H. A., et al. (2019). Effects of tidally varying salinity on groundwater flow and solute transport: Insights from modelling an idealized creek marsh aquifer. *Water Resources Research*, *55*(11), 9656–9672. https://doi.org/10.1029/2018WR024671

Xin, P., Wilson, A., Shen, C., Ge, Z., Moffett, K. B., Santos, I. R., et al. (2022). Surface water and groundwater interactions in salt marshes and their impact on plant ecology and coastal biogeochemistry. *Reviews of Geophysics*, *60*(1), e2021RG000740. https://doi.org/10.1029/2021RG000740

Yuan, R., Zhu, J., & Wang, B. (2015). Impact of sea-level rise on saltwater intrusion in the Pearl River Estuary. *Journal of Coastal Research*, *31*(2), 477–487. https://doi.org/10.2112/JCOASTRES-D-13-00063.1